A Novel Approach for Detection of Illicit Nuclear Activities Using Optically Stimulated Dosimetry

Egemen M. Aras and Robert B. Hayes

North Carolina State University, Burlington Laboratories,
2500 Stinson Dr, Raleigh, NC 27607, United States
E-mail: emaras@ncsu.edu, rbhayes@ncsu.edu

Abstract

The enemy always looks to defeat the detection systems. To handle this tackle, defense in depth in detection is a must. In this work, we propose a complementary detection mechanism for illicit nuclear activities in nuclear facilities in addition to current detection techniques. If one of the detection systems cannot detect illicit nuclear activity, at least one more system is supposed to catch the enemy's action. This action can be either an internal or external thread.

Optically stimulated luminescence dosimetry is used in personal, environmental, retrospective, space, neutron, and medical areas. This system can be a complementary measurement system with the advantages of using without electricity and having those in any nuclear facility. A model is defined with the function of system parameters and the background dose to use OSLDs for the proposed purpose. The model enables us to evaluate the background dose, the initial dose, and the bleaching constant for the reader, including the uncertainty. A case study is worked to prove the model.

According to the model and the case study, we can flag the illicit nuclear activity in the proposed nuclear facility by using optically stimulated luminescence dosimeters (OSLDs).

Keywords: radiation detection; nuclear safeguards; nuclear non-proliferation; optically stimulated luminescence dosimetry

1. Introduction

This work aims to bring a novel approach to detecting illicit nuclear activities using commercially available optically OSLDs produced by LANDAUER® [1], leading to well-known and well-established techniques to determine the dose. OSLDs are used in many fields of radiation dosimetry, including personal, environmental, retrospective, space, neutron, and medical dosimetry [2].

In addition to using a commercial OSLD for retrospective dosimetry, lots of options are available like fired building materials, cementitious building materials, chalk-based plaster, calcium silicate bricks, portable and personal objects, including certain types of telephone cards that contain micro-electronic chips, dental ceramics in the forms of crowns [3]. Moreover, every facility that handles radioactive sources or radiation sources like x-ray above the exempt limit must purchase personal dosimetry services elsewhere. The outcome is that plenty of luminescence materials can be found anywhere; specifically, OSLDs can be found in any facility with a radiation source, including nuclear power plants (NPPs).

Although the ultimate goal of using nuclear technology is to benefit from it by operating for peaceful purposes, someone may turn the nuclear materials into a nuclear weapon. The source of the threat can either be inside or external. This work will focus on trying to address an internal thread in NPPs.

To detect any thread or illicit activity, we need an instrument. This instrument can be used for detection, verification, localization, and identification of the nuclear source and can be pocket-type, hand-held, or fixed installed [4]. Radiation pagers, radiation portal monitors, radioactive isotope identification devices, and radiographic imaging systems are the current detection technologies to detect illicit nuclear activities [5].

An enemy could use various means to defeat detection systems, for example, shielding. The gamma rays from weapons-grade Plutonium are sufficiently energetic and plentiful. They are difficult to shield; however, a layer of lead would shield gamma rays from highly enriched uranium [5]. Background radiation from naturally occurring material, cosmic rays, and even some commercial goods containing

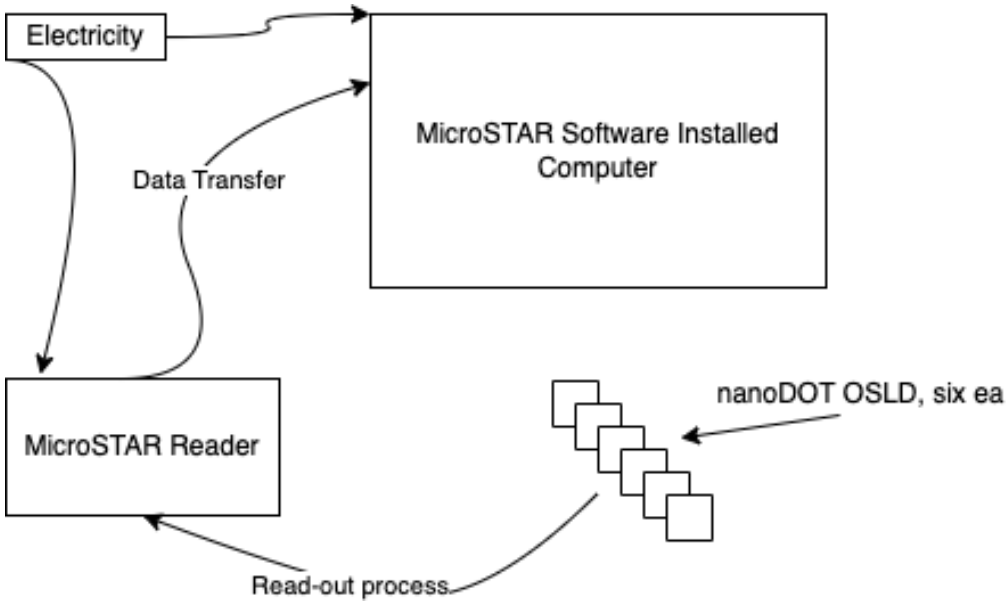

Figure 1: Experimental setup

radioactive material make detection complicated. Multiple detection systems should be used to ensure that the instrumentation system can detect the enemy's activities. For example, if an enemy shields a bomb with a lead, that will create a large, opaque image on a radiograph. Putting a multi-system available can be called defense in depth in detection. In this sense, we proposed a passive measurement method that accompanies the already existing instruments. Our approach will help detect the radiation dose greater than the background and flag the activity as illicit. The approach does not aim to take the place of the current ones; instead, a supportive method that does not require any power during the measurement. Moreover, almost every nuclear facility uses OSLDs to track personal doses.

2. Materials & Methods

The proposed method to flag illicit nuclear activity consists of two steps. The first step is the experimental part, which includes obtaining the background dose, the bleaching constant, and the initial dose to be used in the second part of the study, which is the case study and validation of the proposed method.

The background dose is the amount deposited from the background radiation within the determined time. The bleaching constant is the parameter for the readers that represents how much dose equivalent light is removed with each read-out step. The final result from the first part of the work is the initial dose, the average dose representing the value before the read-out starts.

2.1 Experimental Design and Analysis

The experimental part of the study includes six nanoDOT™ OSLDs produced by LANDAUER® exposed only to background radiation and MicroSTAR® Medical Dosimetry System [1] installed in a regular laptop, as shown in Figure 1.

The consecutive measurements in this system can be done in two different ways, as summarized in Table 1. In addition to getting the necessary values mentioned above, we intend to investigate whether there is a statistically significant difference in different measurement methods or not. A well-known and well-established technique called analysis of variance (ANOVA) is used to compare the results. Details for the ANOVA can be reached elsewhere; however, we follow Chapter 10 of Devore [6].

ANOVA has three primary assumptions, 1) the responses for each factor level have a normal population distribution, 2) these distributions have the same variance, and 3) the data are independent. We test the first condition by looking at the residuals and QQ-Plot of the data, and we know each measurement is independent, which is the third assumption of ANOVA. To check the variance, we have a method called Bartlett's test [7] is used to check whether the measurements have equal variances or not. When the variances are not equal, Welch's ANOVA [8] should be used instead of ANOVA.

The analysis part covers evaluating the dose from the measurement and propagation of uncertainty.

The system does four LED exposure measurements of the dosimeter crystal when conducting a measurement for a nanoDot™ OSLD. It takes the mathematical average to evaluate the expected dose in the unit of mGy. Equation (1) below shows how to assess the average dose. It depends on average raw counts (C), corrected background counts (B), calibration factor (CF) in units counts/dose (mGy), sensitivity (S) as a fractional value, and sensitivity adjustment

Measurement Method	NOREP	REP
Steps for the Measurement	1. Open the system	1. Open the system
	2. Do the calibration	2. Do the calibration
	3. Take one nanoDOT™ OSLD and put it in the reader	3. Take one nanoDOT™ OSLD and put it in the reader
	4. Do measurement	4. Do measurement
	5. Save the result	5. Save the result
	6. Do the same steps (4 and 5) 30 times for every nanoDOT™ OSLD	6. Take the nanoDOT™ OSLD from the reader and
	7. Then take the nanoDOT™ OSLD from the reader	7. Put a new one and do the measurement, save the result and get it back
	8. Put a new nanoDOT™ OSLD to the reader and repeat the steps from 4 to 6	8. Do the same steps (6 and 7) for all six nanoDOT™ OSLDs
	9. Complete measurement	9. When the first measurements are done, do the same procedure 30 times
	10. Get all results from the laptop to analyze	10. Complete measurements
		11. Get all results from the laptop to analyze

Table 1: Road map for two different measurement methods

factor (SAF) is a unitless parameter. The average raw clount is the mathematical average of each dosimeter's four simultaneous measurements. Corrected background counts are obtained as part of the initial instrument start-up process, and the sensitivity adjustment factor is a parameter that the user can modify when needed.

The calibration, which can be done by reading dosimeters with known radiation dose levels and characterizing the relationship between measured raw counts and exposed dose levels, is crucial for any measurements, including the average raw count. So the conversion factor from average raw counts to average dose is called the calibration factor. The sensitivity is the manufacturer's parameter for each dosimeter that refers to the relative light count per dose to the reference nanoDot™.

$$D = \frac{(C) - (B)}{(CF)(S)(SAF)} \tag{1}$$

Each term in Equation (1) contributes to the average dose's uncertainty. First-order uncertainty propagation to Equation (1) gives Equation (2) below.

$$\sigma_D^2 = D^2 \left[\frac{(\sigma_C^2) + (\sigma_B^2)}{(C-B)^2} + \frac{(\sigma_{CF}^2)}{(CF)^2} + \frac{(\sigma_S^2)}{(S)^2} + \frac{(\sigma_{SAF}^2)}{(SAF)^2} \right] \tag{2}$$

The average net count uncertainty $\sigma_N^2 = \sigma_C^2 + \sigma_B^2$ can be used in Equation (2), calculated as the standard deviation of four follow-up measurements for each dosimeter per measurement step. Although no method is applied to correct either background counts or SAF in this study, it is assumed that B's uncertainty was 1. The uncertainty on SAF is 0.01 since the software does all calculations by setting B as 0 and SAF as 1.00, respectively. The chosen uncertainty is based on significant digits given by the software. The parameter related to manufacturing, S, is specific for each dosimeter though similar to all others. However, S's uncertainty is assumed to be the same for each dosimeter, that is, 0.01 as a fractional value. The sensitivity takes a value of either 0.92 or 0.96, which justifies our assumption is valid for the uncertainty on S. The conversion factor from counts to dose in the units of counts/dose (mGy), named calibration factor, has two values: low dose measurement and high dose measurement. The uncertainty is 0.001 for low dose measurement, which is our concern in this work. The calibration factor for low dose measurement is 408.081 for our case given by the software.

2.2 Case Study and Validation

A scenario is developed to verify our proposed method. According to the scenario, a single used ^{235}U fuel assembly in a corridor with the assumed positions and geometry as shown in Figure 2. Angle 1 is θ, and Angle 2 is φ in our calculations. The nanoDOT™ OSLD is located in the wall of the corridor. The detail for the scenario is that it is used for 30,000 hours, has a thermal power of 20 MW, then removed from the service and placed in storage for one year.

The goal is to evaluate the dose rate at a 5 meters distance for unshielded and shielded with concrete circumstances. Although the numbers are subject to change from facility to facility, the calculation method is supposed to be identical.

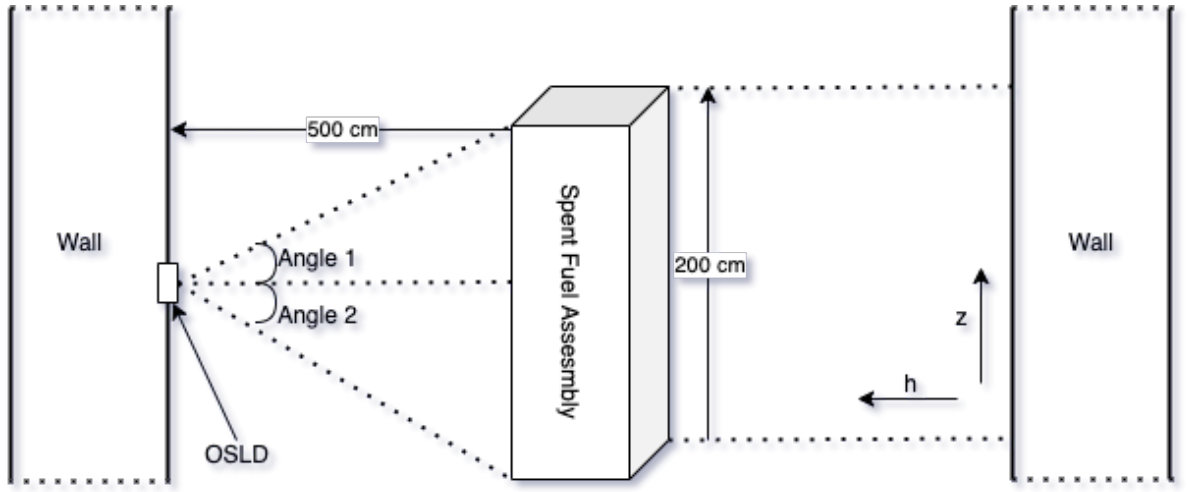

Figure 2: An example case for applying nanodot OSLD as a detector for flagging illicit nuclear activity

Evaluating dose rate with the given conditions [9] will follow the evaluation steps listed below:

1. Source strength (S)
2. Unshielded - uncollided gamma-dose rate (D0)
3. Shielded gamma-dose rate (D)

The calculation starts with Equation (3) by the evaluating $\Gamma_j(t_0, t_s)$ [MeV/fission] is the rate of energy release in group j at time t_s (sec) following an operation at a constant fission rate (sec^{-1}) for time t_0(sec). i is the number of parameters listed for a_{ij} (MeV/sec) and λ_{ij} (s^{-1}). The average energy in each group is assumed as the arithmetic average of the range provided in the same table. The data used for calculation is available in Appendix G.1 of Shultis & Faw [10]. P_0 (fission/sec) is evaluated assuming that 200 MeV energy is released per fission and N_j is the group number.

$$\Gamma_j(t_0, t_s) = P_0 \sum_{i=1}^{N_j} \frac{a_{ij}}{\lambda_{ij}} e^{-\lambda_{ij} t_0} [1 - t_s] \tag{3}$$

We ignore the attenuation and build-up in the air while evaluating the dose rate as given in Equation (4). The response function can be assessed as seen in Equation (5) by applying Appendix C.7 of Shultis & Faw [10] for the $\left(\frac{\mu_{en}}{\rho}\right)_{tissue}$. Note that a point source is moved between two positions along a line at a constant rate that would be equivalent to a linear source of the same total activity distributed over the travel distance.

$$D^0(P) = \frac{1}{4\pi h} \sum_{i=1}^{6} S_{l,i} R_i \left[\tan^{-1}\left(\frac{200 - z}{h}\right) + \tan^{-1}\left(\frac{z}{h}\right) \right] \tag{4}$$

$$with \begin{cases} \theta = \tan^{-1}\left(\frac{200 - z}{h}\right) \\ \varphi = \tan^{-1}\left(\frac{z}{h}\right) \end{cases}$$

$$R = 1.602x10^{-10} E \left(\frac{\mu_{en}}{\rho}\right)_{tissue} \tag{5}$$

When considering shielding material between the source and the detector, the data for the parameters $A1$, $A2$, $\alpha 1$, and $\alpha 2$ is taken from Table E.5 of Shultis & Faw [10] for Equation (6).

$$D(t) = \frac{1}{2\pi h} \sum_{j=1}^{6} S_{l,i} \bar{R}_J \sum_{i=1}^{2} A_{i,j} F\left(\theta, \left[1 + \alpha_{i,j}\right] \mu_j t\right) \tag{6}$$

3. Results & Discussion

This section has two main pillars; in the first pillar, we present experimental results with the statistical analysis, and in the second pillar, we present the case study results.

3.1 Experimental Results with Statistical Analysis

We have thirty measurements for each method mentioned in Table 1. In addition to comparing these two measurements, we also use a complete set of sixty measurements as a one-batch measurement dupped as ALL, and we compare NOREP, REP, and ALL measurements.

The average trap population's expected behavior in terms of light output per read-out is given in Equation (7) and depends on the number of read-outs n. Here, m1 is the total noise, and m2 is the bleaching constant.

$$\frac{dD(n)}{dn} = m_1 - m_2 D(n) \tag{7}$$

The solution of this Equation, given in Equation (8), provides a fitting function for the experimental data set. The new parameter m3 is the initial dose in Equation (8), representing the dose before any read-out. Moreover, m1/m2 is the background dose, one of the main outputs of this experiment.

$$D(n) = \frac{m_1}{m_2} - \left(m_3 - \frac{m_1}{m_2}\right) e^{-m_2 n} \tag{8}$$

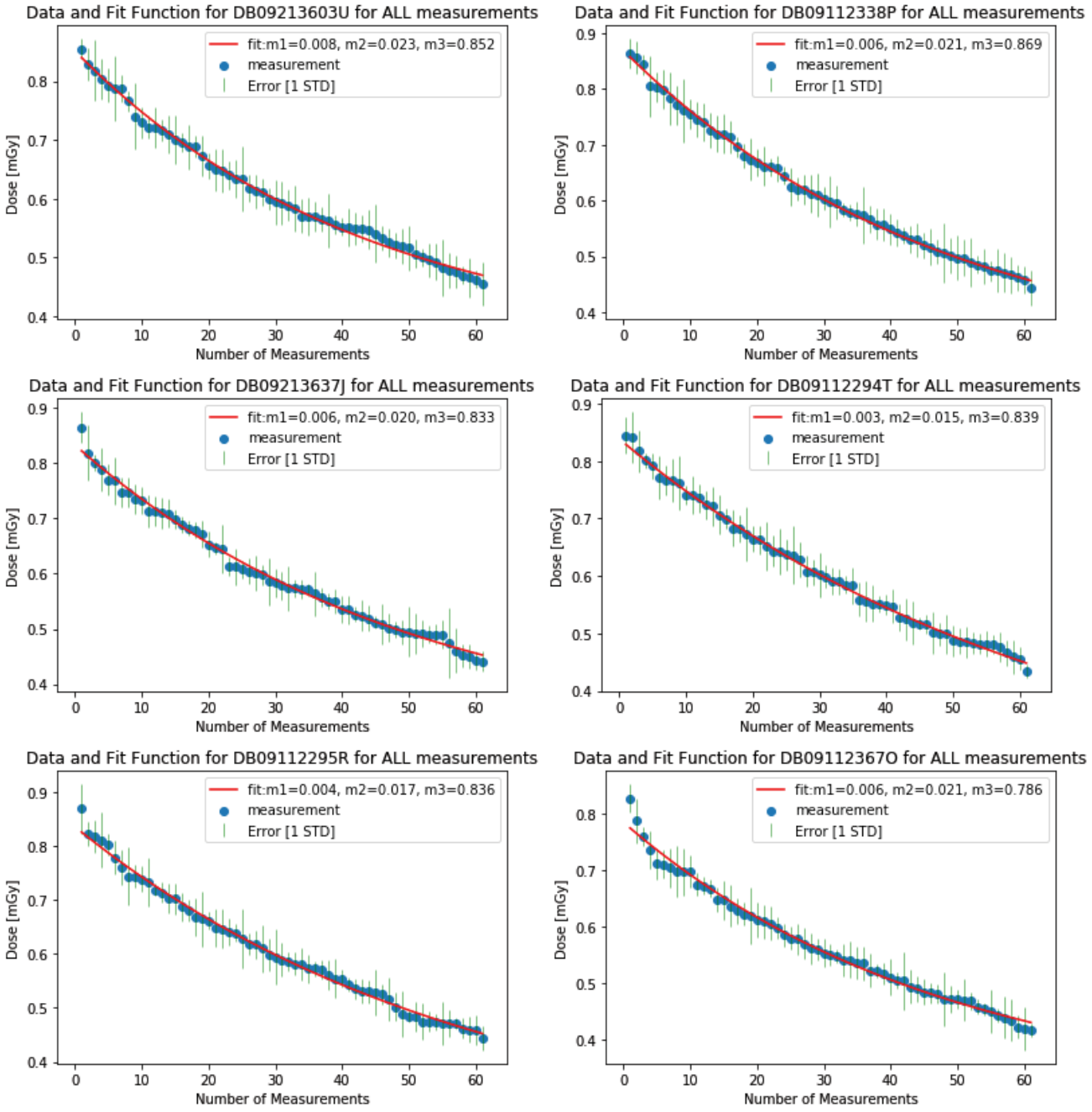

Figure 3: All measurements for six nanoDOT™ OSLD, including uncertainty and fitting model

Figure 3, Figure 4, and Figure 5 show the measurements and fit function for the measurement set, including uncertainty, for six nanoDot™ OSLD dosimeters. These include the whole set, the without removal set, and the removed set, respectively. Combining experimental results with Equation (8) gives background dose, bleaching constant, and initial dose with the uncertainty for six nanoDOT™ OSLD for two measurement methods and all measurements.

The background dose rate is assumed constant during the measurement. The obtained result for the background dose is shown in Table 2.

#	Bkg dose-All [mGy]	Bkg dose-NoRep [mGy]	Bkg dose-Rep [mGy]
1	0.345±0.034	0.424±0.077	0.750±0.114
2	0.298±0.022	0.264±0.139	0.282±0.066
3	0.293±0.045	0.082±0.289	0.151±0.294
4	0.189±0.039	0.279±0.123	0.267±0.188
5	0.242±0.046	0.338±0.164	0.359±0.101
6	0.294±0.042	0.440±0.122	0.035±0.250

Table 2: Evaluated background dose [m1/m2] for each dosimeter and each experiment part

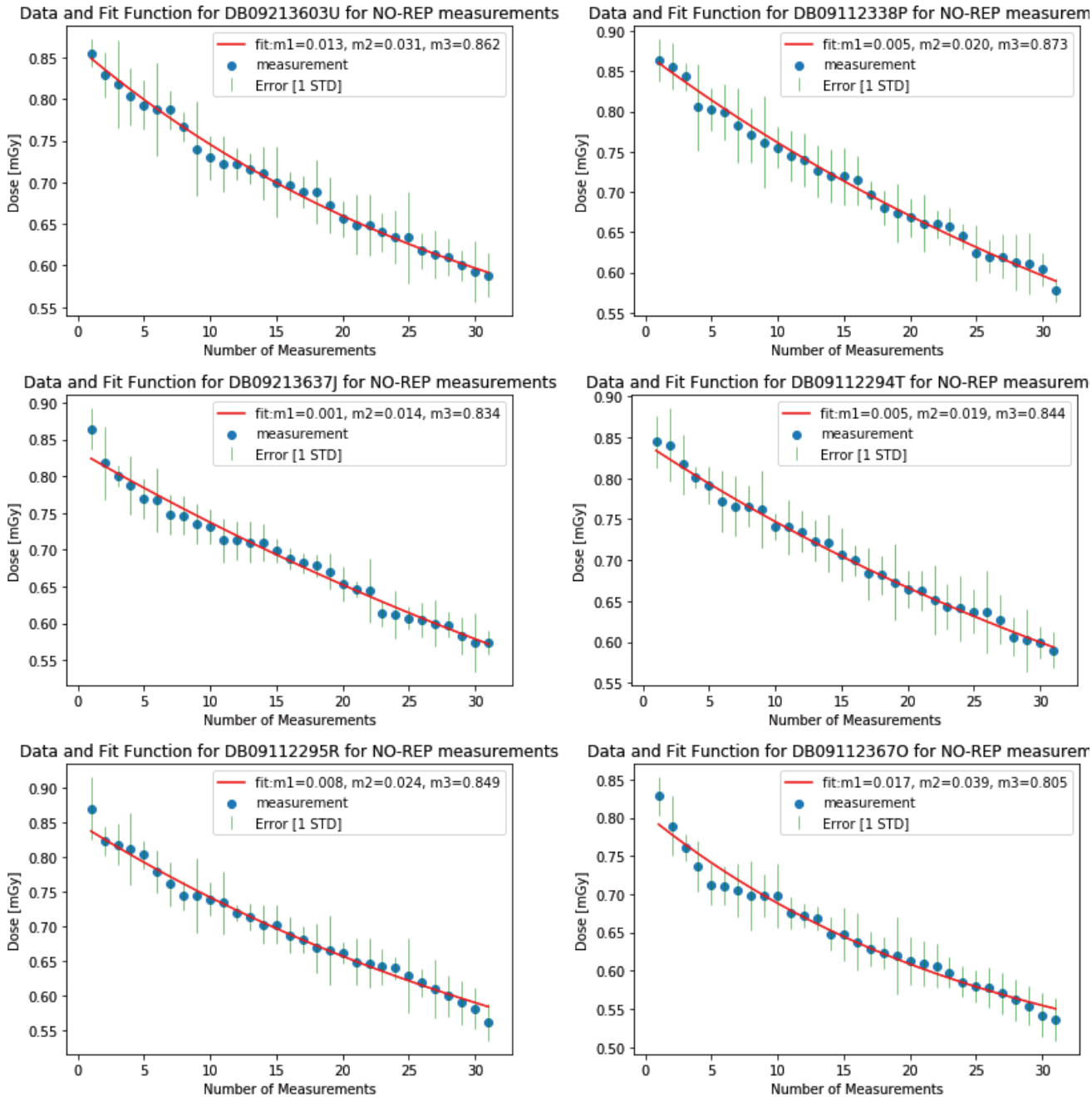

Figure 4: Measurements for six nanoDOT™ OSLD, NOREP method, including uncertainty and fitting model

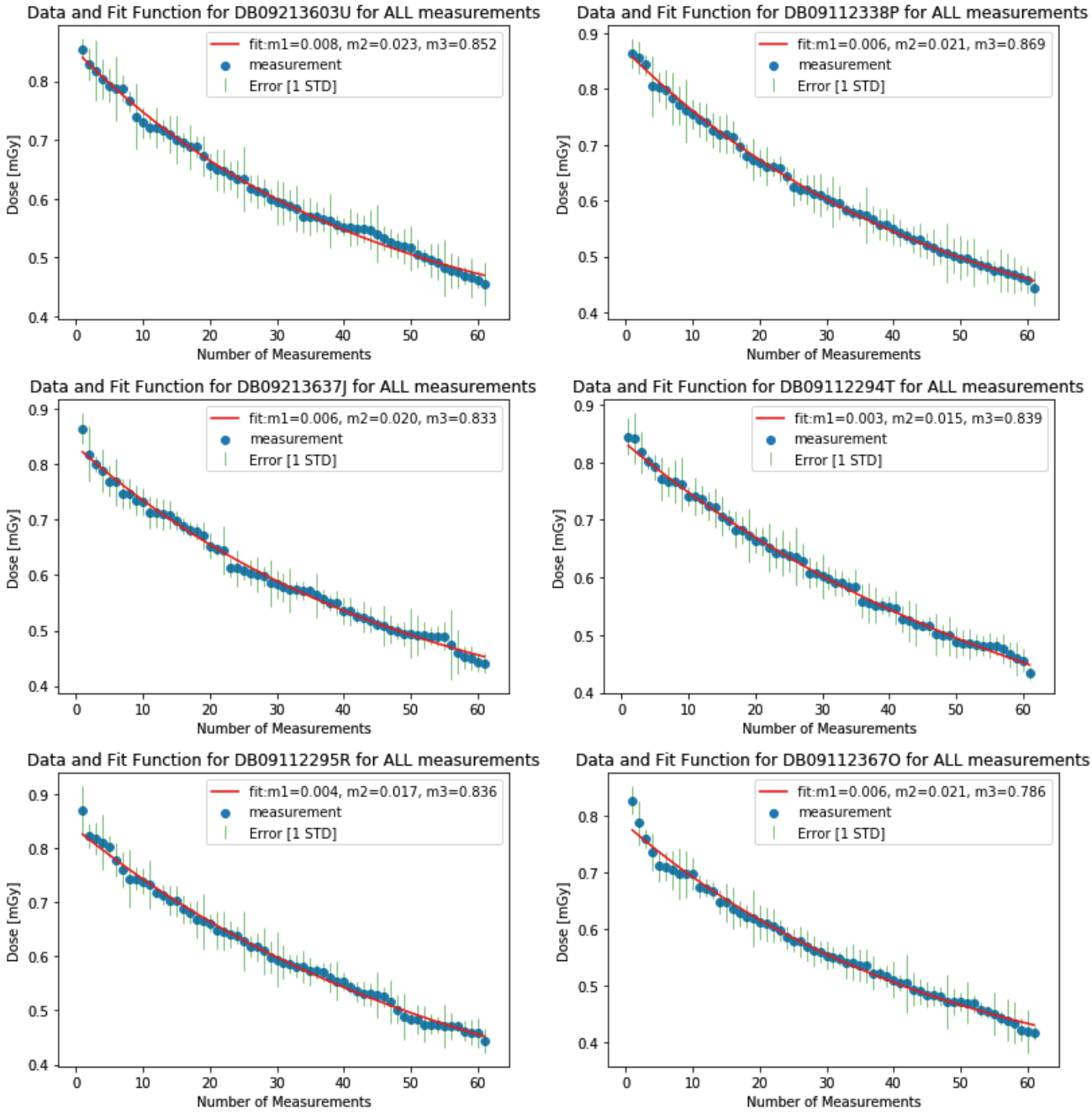

Figure 5: Measurements for six nanoDOT™ OSLD, NOREP method, including uncertainty and fitting model

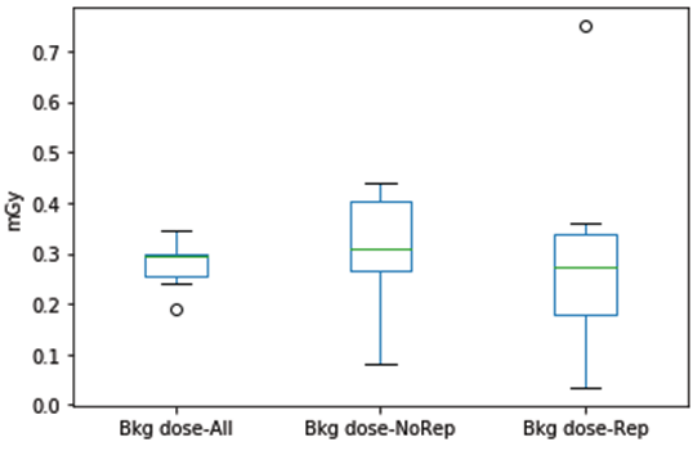

Figure 6: Comparison of background dose values for each case.

The first goal is to compare the REP, NOREP, and ALL results by applying ANOVA. Table 2, Table 3, and Table 4 are the results for the background dose, the bleaching constant, and the initial dose, respectively. According to Figure 7, Figure 9, and Figure 11, the residuals are normally distributed with a mean zero that obeys the first assumption of the ANOVA. Moreover, all the measurements are independent, meaning that the second assumption for ANOVA is also satisfied. On the other hand, the Bartlett test [7] for each parameter suggests that the variances are not homogeneous. Welch's ANOVA applies to the data set instead of ANOVA. As a result of Welch's ANOVA, we fail to reject the null hypothesis that the background dose, the bleaching constant, and the initial dose are equal. These leads using

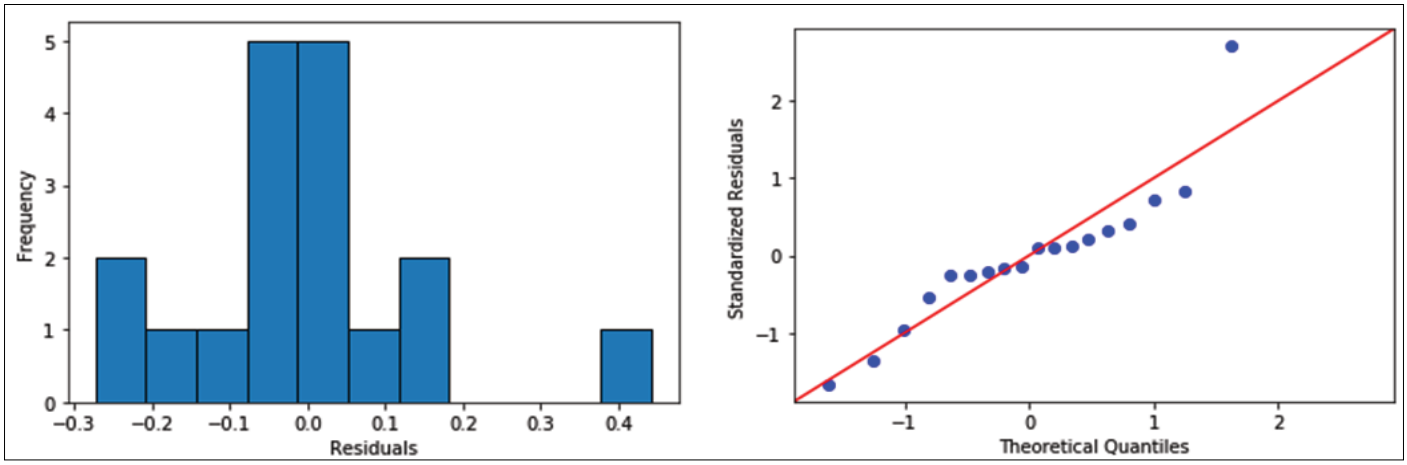

Figure 7: Histogram of residuals and QQ plot for background dose ANOVA analysis

#	Bleaching constant -All [1/read-out]	Bleaching constant -No Rep [1/read-out]	Bleaching constant -Rep [1/read-out]
1	0.023±0.001	0.031±0.003	-0.020±0.004
2	0.021±0.001	0.020±0.004	0.021±0.003
3	0.020±0.002	0.014±0.006	0.013±0.008
4	0.015±0.001	0.019±0.003	0.021±0.008
5	0.017±0.001	0.024±0.006	0.035±0.007
6	0.021±0.002	0.039±0.007	0.010±0.005

Table 3: Evaluated bleaching constant [m2] for each dosimeter and each experiment part

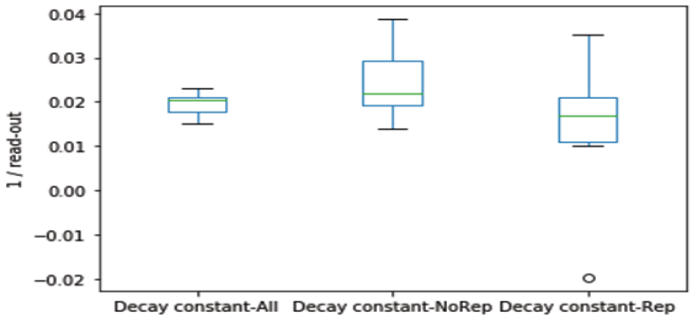

Figure 8: Comparison of bleaching constant values for each case

either REP or NOREP methods for measurement do not have a statistically significant difference.

Figure 6, Figure 8, and Figure 10 are for the comparison of the evaluated parameters. In every box plot, we have an outlier for the REP method. This region was the second suite of measurements so it would have been the most bleached. If it were sufficiently flat, an exponentially decaying exponential with sufficient noise can have the best fit give it a negative slope, just as would occur with a linear fit.

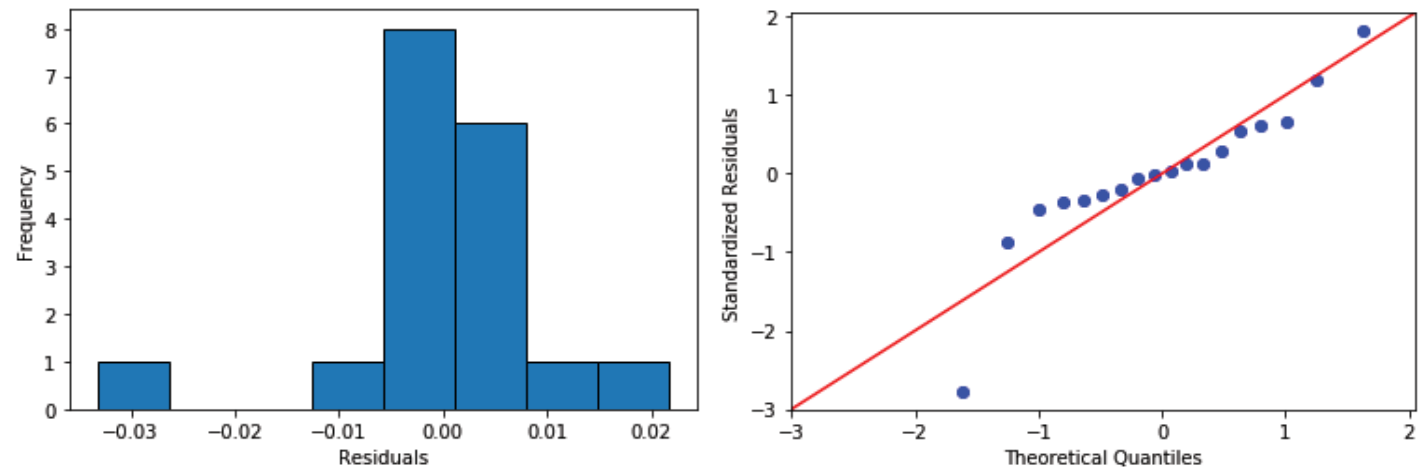

Figure 9: Histogram of residuals and QQ plot for bleaching constant ANOVA analysis

#	Initial dose -All [mGy]	Initial dose - NoRep [mGy]	Initial dose - Rep [mGy]
1	0.852±0.004	0.862±0.004	0.660±0.002
2	0.869±0.003	0.873±0.005	0.892±0.001
3	0.833±0.005	0.834±0.007	0.803±0.004
4	0.839±0.003	0.844±0.003	0.893±0.005
5	0.836±0.004	0.849±0.006	1.111±0.005
6	0.786±0.005	0.805±0.008	0.749±0.003

Table 4: Initial dose values for each case

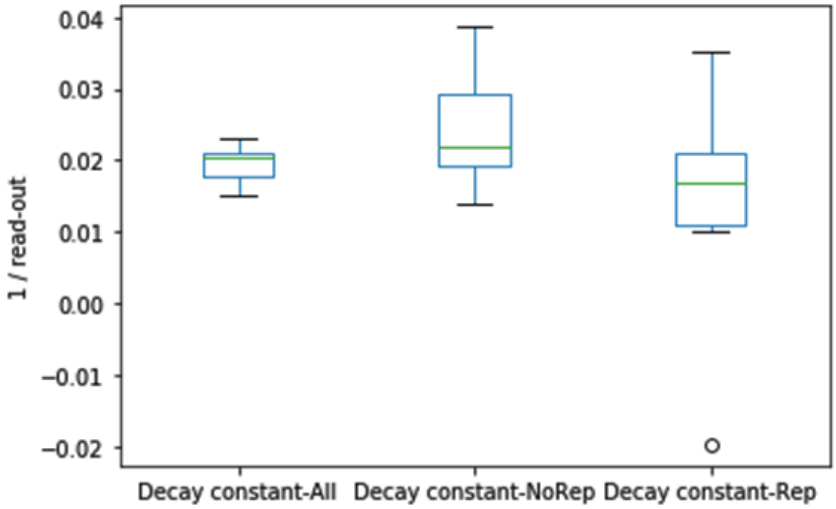

Figure 10: Comparison of bleaching constant values for each case

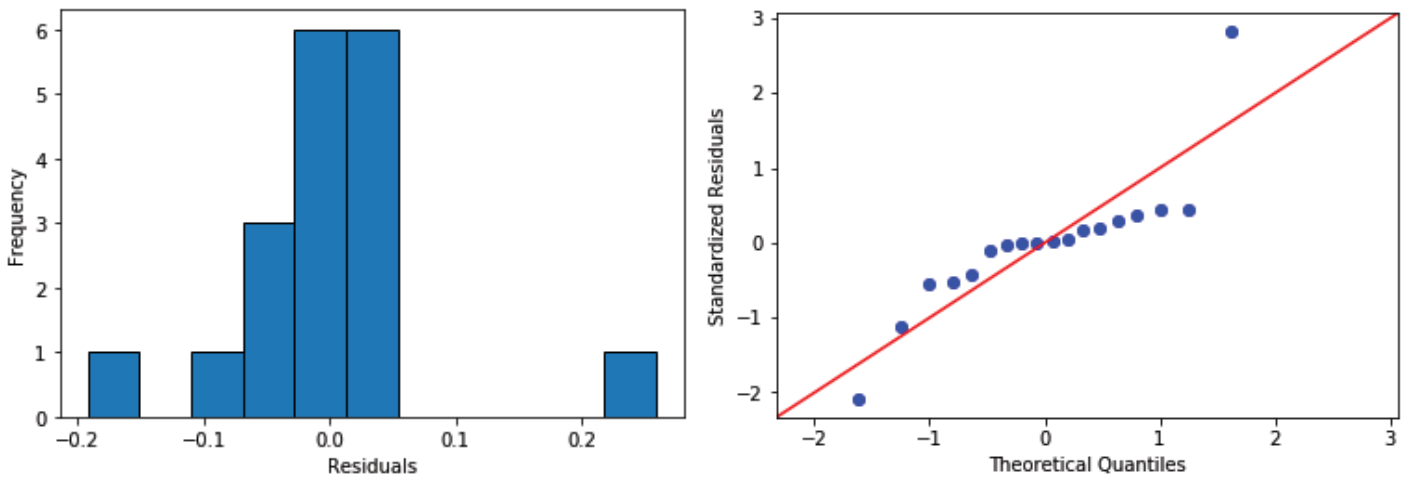

Figure 11: Histogram of residuals and QQ plot for initial dose ANOVA analysis

Energy [Mev], [1]	Kappa [Mev/sec] [2]	Average Energy [MeV] [3]	Kappa [photons/sec] [4]=[2]/[3]	Source Strength [photons/cm-sec] =[4]/[Length]
Group 1 [5-7.5]	5.1E+02	6.25	8.2E+01	4.1E-01
Group 2 [4-5]	3.93E+06	4.5	8.7E+05	4.4E+03
Group 3 [3-4]	1.98E+08	3.5	5.7E+07	2.8E+05
Group 4 [2-3]	2.35E+14	2.5	9.4E+13	4.7E+11
Group 5 [1-2]	9.99E+13	1.5	6.7E+13	3.3E+11
Group 6 [0-1]	4.61E+15	0.5	9.2E+15	4.6E+13

Table 5: Evaluated source strength for each group

3.2 Results of Case Study

The source strength for each group is evaluated as an initial step in Table 5.

Using the source strength, we obtain the uncollided - unshielded dose per length of the spent fuel assembly given in Table 6. Group 6 is responsible for more than 90% of the total dose rate. We ignore other groups' contributions to the dose rate for the remaining calculations.

Figure 12 shows the uncollided – unshielded dose rate for Group 6 only with the function of the spent fuel assembly's height. As expected, the maximum dose rate at the center is about 8.2 mGy/sec, much more than the background dose of about 0.3 mGy.

Figure 13 is the final result that we intend to obtain, the total dose rate for the concrete shielded spent fuel. As shielding thickness increases, the dose rate decreases as a function of the thickness of the shield. The total gamma-dose rate is about one mGy per second beyond the 22 cm concrete shield, which is even distinguishable from the approximate background dose, about 0.3 mGy.

Energy [Mev]	Average Energy [MeV]	Source Strength [photons/cm-sec]	(μen/ρ)tissue [cm^2/g]	Response Function [$Gy\text{-}cm^2$]	SI*R [Gy-cm]
Group 1 [57.5]	6.25	4.1E-01	1.77E-02	1.77E-11	7.2E-12
Group 2 [4-5]	4.5	4.4E+03	1.97E-02	1.42E-11	6.2E-08
Group 3 [3-4]	3.5	2.8E+05	2.15E-02	1.21E-11	3.4E-06
Group 4 [2-3]	2.5	4.7E+11	2.42E-02	9.69E-12	4.6E+00
Group 5 [1-2]	1.5	3.3E+11	2.81E-02	6.74E-12	2.2E+00
Group 6 [0-1]	0.5	4.6E+13	3.27E-02	2.62E-12	1.2E+02
TOTAL					1.3E+02

Table 6: Calculated uncollided dose rate as a function of the length of the spent fuel assembly

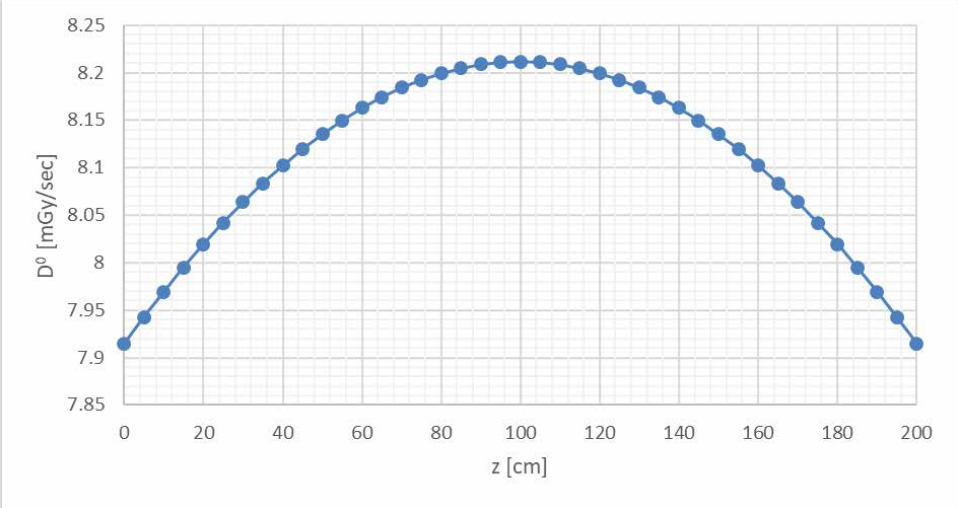

Figure 12: Dose rate distribution of spent fuel assembly for uncollided and unshielded case

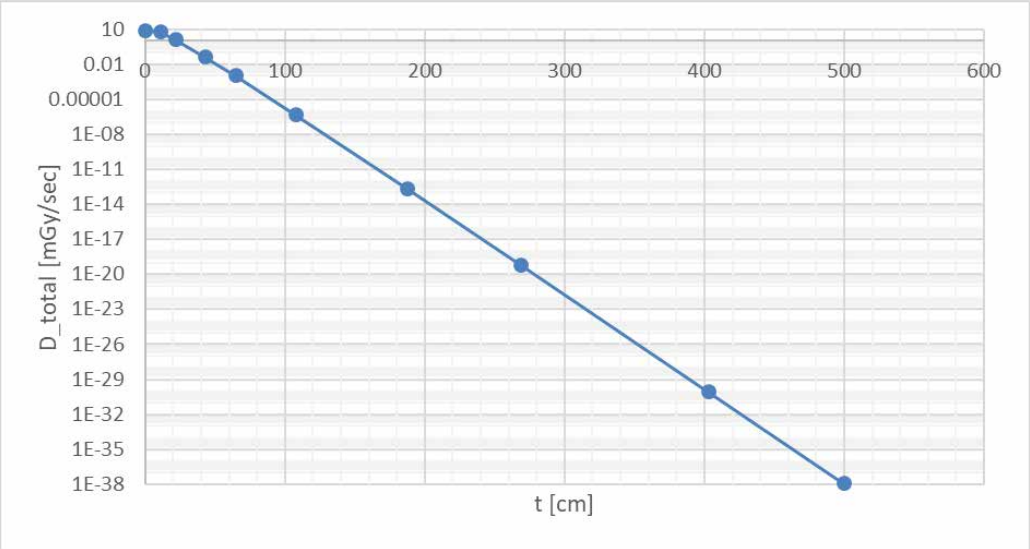

Figure 13: Total gamma dose rate for different shielding thickness

4. Conclusion

We propose a model to flag the illicit nuclear activities in nuclear facilities by using OSLDs as a complementary system to current detection systems.

We first set an experiment to obtain model variables to make the model work. Then we demonstrate a case study on a used nuclear fuel assembly in unshielded and concrete shielded cases to prove our model.

The result of this work allows us to get the background dose, the bleaching constant for the reader, and the initial dose with their uncertainties as a first step. The first step enables us to demonstrate our scenario. In the end, we flag the illicit nuclear activity in the proposed facility.

As follow-up work, we plan to redo the experimental part by using OSLDs from the same producer exposed to a high radiation level of more than 500 mGy. This high dose level will prove the model more realistically. The follow-up work will allow us to generalize our model for nuclear facilities. Some specific cases are intended to be picked as a scene rather than traditional light water reactors' spent fuel as additional works.

5. Acknowledgements

This work is a follow-up work to Egemen M. Aras's master thesis. Egemen M. Aras is funded by the Ministry of National Education of Turkey during his master's.

6. References

[1] Landauer, "MicroSTAR User Manual." Landauer, 2019. [Online]. Available: https://www.landauer.com/sites/default/files/2020-01/MICROSTAR%20ii%20USER%20MANUAL.pdf

[2] S. W. S. McKeever, *"Optically stimulated luminescence: A brief overview,"* Radiation Measurements, vol. 46, no. 12, pp. 1336–1341, Dec. 2011, doi: 10.1016/j.radmeas.2011.02.016.

[3] H. Y. Göksu and I. K. Bailiff, *"Luminescence dosimetry using building materials and personal objects," Radiation Protection Dosimetry*, vol. 119, no. 1–4, pp. 413–420, Sep. 2006, doi: 10.1093/rpd/nci699.

[4] International Atomic Energy Agency, Ed., *Detection of Radioactive Materials at Borders.* Vienna: IAEA, 2003.

[5] J. Medalia, *"Detection of Nuclear Weapons and Materials: Science, Technologies, Observations,"* Congressional Research Service, R40154, Jun. 2010.

[6] J. L. Devore, *Probability and statistics for engineering and the sciences.* Boston, MA: Boston, MA : Cengage Learning, [2016], 2016.

[7] G. W. Snedecor and W. G. Cochran, *Statistical Methods.* Ames: Ames : Iowa State University Press, [1967], 1967.

[8] H. Liu, "Comparing Welch's ANOVA, a Kruskal-Wallis test and traditional ANOVA in case of Heterogeneity of Variance," Master of Science Thesis, Virginia Commonwealth University, Richmond, Virginia, 2015.

[9] R. J. LaBauve, T. R. England, D. C. George, and C. W. Maynard, "Fission Product Analytic Impulse Source Functions," *Nuclear Technology,* vol. 56, no. 2, pp. 322–339, Feb. 1982, doi: 10.13182/NT82-A32861.

[10] J. K. Shultis and R. E. Faw, *Radiation Shielding*. La Grange Park, IL: La Grange Park, IL : American Nuclear Society, [2000], 1996.